Mon. Not. R. Astron. Soc. **000**, 1–10 (2002) Printed 1 February 2008 (MN LATEX style file v1.4)

What regulates the velocity distribution of interstellar clouds?

Massimo Ricotti[1] and Andrea Ferrara[2]
[1] *Center for Astrophysics and Space Astronomy University of Colorado, Boulder, CO 80309*
[2] *Osservatorio Astrofisico di Arcetri Largo E. Fermi, 5 - 50125 Firenze, Italy*

ABSTRACT
Kinetic energy stored in ISM bulk/turbulent motions is a crucial ingredient to properly describe most properties of observed galaxies. By using Monte Carlo simulations, we investigate how this energy is injected by supernovae and dissipated via cloud collisions and derive the corresponding ISM velocity probability distribution function (PDF). The functional form of the PDF for the modulus of the velocity dispersion is

$$p(v) \propto v^2 \exp[-(v/\sigma)^\beta].$$

The power-law index of the PDF depends only on the value of the average cloud collision elasticity $\langle\epsilon\rangle$ as $\beta = 2\exp(\langle\epsilon\rangle - 1)$. If β and the gas velocity dispersion σ are known, the specific kinetic energy dissipated by collisions is found to be $\propto \sigma^2 \ln(2/\beta)/(\beta - 0.947)$; in steady state, this is equal to the energy input from SNe. We predict that in a multiphase, low metallicity ($Z \approx 5 \times 10^{-3} Z_\odot$) ISM the PDF should be close to a Maxwellian ($\beta = 2$) with velocity dispersion $\sigma \gtrsim 11$ km s^{-1}; in more metal rich systems ($Z \gtrsim 5 \times 10^{-2} Z_\odot$), instead, we expect to observe almost exponential PDFs. This is in good agreement with a number of observations that we review and might explain the different star formation modes seen in dwarfs and spiral galaxies.

Key words: Hydrodynamics – Shock waves – ISM: kinematics and dynamics

1 INTRODUCTION

An increasing number of recent studies have come to the conclusion that a large, if not dominant, fraction of the energy injected into the interstellar medium (ISM) in various forms by stellar activity, resides in bulk/turbulent motions of the gas (e.g. McKee 1990, Lockman & Gehman 1991, Ferrara 1993, Vazquez-Semadeni *et al.* 1995, Norman & Ferrara 1996 [NF]). Energy in this form is required, for example, to reproduce the observed vertical distribution of the HI in the Galactic disk. The corresponding turbulent pressure is estimated to be from $\geqslant 8$ (McKee 1990) to $\simeq 30$ (NF) times larger than the thermal one. Note that such large ratios imply a high porosity factor, Q, of the hot gas produced by supernova (SN) explosions: McKee (1990) estimates that $Q \sim 1.1(P_{turb}/P_{tot})^{4/3}$. This dynamical property of the ISM has a dramatic importance in shaping the resulting structure of the parent galaxy. A number of numerical models (Vázquez-Semadeni *et al.* 1995, 1998; Ballesteros-Paredes *et al.* 1999; Korpi *et al.* 1999) have been developed in order to describe the global properties of a turbulent ISM in the Galaxy improving on the pioneering works by Rosen *et al.* (1993, 1996) and Rosen & Bregman (1995). Although these studies provide a first approach to the study of the ISM properties on galactic scales, finite resolution limits their ability to properly describe shocks arising both as a consequence of SN explosions and cloud collisions, thus making their estimates of the kinetic energy dissipation rather uncertain. The same caveat should be made for the treatment of thermal instabilities (and hence cloud formation) which requires to spatially resolve the "Field length" (Hennebelle & Perault 1999). Galaxy formation studies in a cosmological context (Katz 1992, Mihos & Hernquist 1994, Navarro & Steinmetz 2000, Springel 2000), have by now firmly established that star formation cannot be properly regulated by forcing a phase transition of the gas into the hot phase by thermal energy input from SN explosions alone. Current computational power limits the spatial and the time scale resolution of the simulations, implying a too highly dissipative treatment. Moreover small-scale physical processes usually cannot be modeled with sufficient detail. A surprisingly

better description of galactic disk properties is obtained once an heuristic equation of state for the ISM is assumed with parameters adjusted to simulate the effects of a turbulent pressure. In these models a fraction of the available energy is invested in modifying the kinetic energy of the gas (Navarro & Steinmetz 2000). The recipe for this approach is relatively simple and it constitutes a promising path to understand galaxy formation, but it needs to be calibrated against well known situations as for example the Galactic ISM, where a large number of high quality observations on the HI dynamics are available. Finally, Ferrara & Tolstoy (2000) point out that if energy injection is mainly regulated by massive stars, then the observed metallicity range of galaxies must be consistent with what inferred from the ISM kinetic energy budget. Along these lines they find that a tight relation between gas velocity dispersion and metallicity in dwarfs must exist.

In view of the above situation, we have decided to explore how kinetic energy is injected by SN explosions and radiated away as converging gas flows collide at supersonic velocities. The present work is mainly building on previous investigations by our group which have concentrated on the analysis of high-res hydro- and MHD simulations of cloud collisions (Ricotti, Ferrara & Miniati 1997 [RFM], Miniati *et al.* 1997, 1999). The main effort there was devoted to quantify the amount of kinetic energy dissipation as a function of the collision parameters and cloud properties. Here we take a more global, although simplified, approach to understand the interplay between the two above mentioned processes (SN explosion and cloud-cloud collisions) regulating the dynamics/energetics of the turbulent ISM. To this aim, we will adopt a statistical description based on a Monte Carlo approach that allows us to derive a probability distribution function (PDF) for the ISM velocity dispersions. The PDF is then shown to hold directly measurable and easily interpreted information about the kinetic energy regulation in the ISM.

The paper is organized in the following manner. In § 2 we discuss our statistical approach to the modeling of a turbulent ISM and the model assumptions. In § 3 we present the results. In § 4 we show that our results are in agreement and can explain a number of observational results, that we review, from published literature. In § 5 we justify the simple assumptions of our model and in § 6 we summarize the results.

2 MODEL ASSUMPTIONS

We consider a galaxy of total HI mass M_{CNM} distributed in clouds of mass M_c and cloud filling factor f_c. The clouds constituting the Galactic Cold Neutral Medium (CNM) phase have typically a gas number density $n_c = \rho_c/\mu m_p \sim 50$ cm^{-3}, where μ is the mean molecular weight and m_p the proton mass. If the clouds are further idealized as homogeneous spheres of radius R_c, the total number of clouds is $N_{tot} = M_{CNM}/M_c$. The cross section for cloud collisions is $A = \mathcal{B}\pi R_c^2$, where the unknown parameter $\mathcal{B} \sim 1$ takes into account the effect of magnetic field, tidal forces and gravitational focusing, effective at low (5-6 km s^{-1}) cloud relative velocities (Lockman & Gehman, 1991). It follows that the number density of clouds is $\mathcal{N}_c = 3N_{tot}f_c/4\pi R_c^3$, and their collisional frequency $\nu = \mathcal{N}_c A \overline{v}_r$, where $\overline{v}_r$ is the mean relative velocity of colliding clouds.

We use a set of Monte Carlo simulations to model the dynamics/dissipation of cloud collisions, and the energy input from SN explosions and stellar winds. We assume a homogeneous and isotropic spatial distribution of the clouds and energy sources. In this case, the system is completely characterized by the evolution of the velocity probability distribution function (PDF) for the modulus of the velocity of the clouds, which in case of a Maxwellian distribution can be expressed as,

$$p(v) \propto v^2 \exp\left(-\frac{v^2}{\sigma^2}\right) , \quad (1)$$

where the 3D velocity dispersion, σ, is related to the observed 1D velocity dispersion by the relationship, $\sigma = \sqrt{3}\sigma_{1D}$.

Starting from an initial PDF (typically a Maxwellian), we evolve the distribution at subsequent time steps $\Delta t = (\nu N_{tot})^{-1}$ as follows. At each time step we select two clouds (we do not consider three body encounters) from the velocity distribution, with initial velocities $v_{1,i}$ and $v_{2,i}$, by randomly sampling the PDF and calculate the final velocities $v_{1,f}$ and $v_{2,f}$ after the collision. The expression for the new velocities are

$$v_{1,f}^2 = v_r^2 + v_{cm}^2 - 2v_r v_{cm}\cos\varphi \ ; \quad (2)$$

$$v_{2,f}^2 = v_r^2 + v_{cm}^2 + 2v_r v_{cm}\cos\varphi \ , \quad (3)$$

where the relative velocity after the collision and the center of mass velocities are, respectively:

$$v_r^2 = \frac{\epsilon}{2}[v_{1,i}^2 + v_{2,i}^2 - 2v_{1,i}v_{2,i}(\sin\theta\cos\phi + \cos\theta\sin\phi\cos\varphi)] \ ; \quad (4)$$

$$v_{cm}^2 = \frac{1}{2}[v_{1,i}^2 + v_{2,i}^2 + 2v_{1,i}v_{2,i}(\sin\theta\cos\phi + \cos\theta\sin\phi\cos\varphi)] \ ; \quad (5)$$

$\epsilon(v_{r,i}, R_c, Z)$ is the elasticity of the collision, with $v_{r,i}$ being the relative velocity before the collision (see discussion in § 2.1.2) and Z the gas metallicity. For the definition of the angles θ, φ, ϕ see the sketch in Fig. 1.

Every $\gamma = (\nu_{SN}\Delta t)^{-1}$ collisions, where ν_{SN} is the SN rate in the galaxy, an energy $E = \kappa E_{SN}$ is added to the system; $E_{SN} = 10^{51}$ erg is the total energy of the SN explosion and $\kappa = 0.02$ is the fraction* converted in kinetic energy of the engulfed clouds (Thornton *et al.* 1998). As long as cloud coagulation, cloud destructions or formations are neglected in the model, the following simple argument suggests that the cloud collision rate, ν, is constant. The scale height of the gaseous disk in galaxies is $H \propto \overline{v}_r$ (McKee 1990, Ferrara 1993). Since in our model we assume constant gas mass and cloud mass (*i.e.* , $N_{tot} = const.$, at least in a statistical sense) we have $\mathcal{N}_c \propto \overline{v}_r^{-1}$. It follows from the definition of ν, given at the beginning of this paragraph, that ν is constant. If, in addition, we assume constant SN explosion rate we

* The adopted value of the coefficient κ is perhaps controversial because based on 1D hydro-simulations. In a more realistic model dynamical instabilities and turbulence could play a crucial role. We do not worry about this uncertainty because the qualitative results of this paper are unaffected by a different choice of κ.

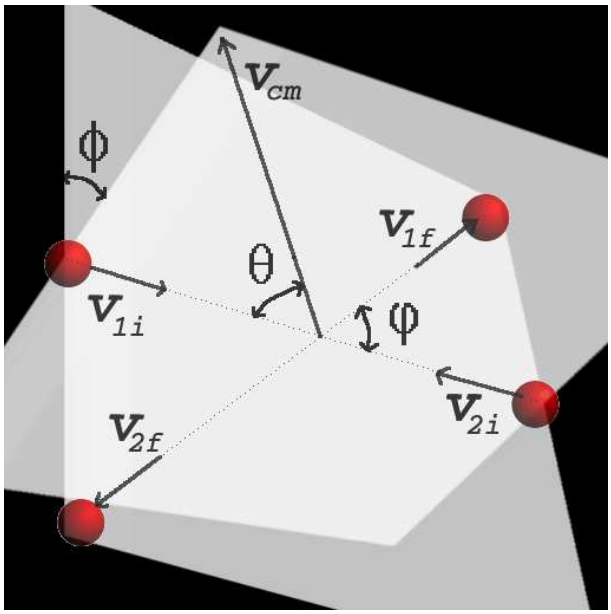

Figure 1. Sketch of the collision geometry and angle definitions.

have $\gamma = const.$ since $\Delta t = (\nu N_{tot})^{-1}$ and N_{tot} is constant. To summarize, the model is characterized by four constant parameters which must be appropriately chosen to describe the galaxy under study: M_c, R_c, Z and γ. Note that in a self-consistent global model of the ISM these four parameters are not independent but correlated. Here we are not interested in a global modeling of the ISM that would require a different approach to the problem using high resolution hydro- simulations. Therefore we rely on observational and theoretical results found in literature to determine a range of realistic values for those parameters.

2.1 Energy sources and sinks

2.1.1 Turbulent pumping by supernova explosions

The main source of the kinetic energy required to support the observed HI bulk motions in the Galaxy is provided by SN explosions and stellar winds (McKee 1990, NF). The latter authors calculated the source function for interstellar turbulence by using a detailed formalism to account for the interaction between SN shock waves and the clouds, which are thereby accelerated and put into motion. For brevity, we only repeat here the main results relevant to this study, deferring the interested reader to NF for further details.

To simplify our treatment we only consider primary shocks, *i.e.* shocks associated with the SN explosion itself, as a source of kinetic energy for the clouds. Therefore we neglect secondary shocks, *i.e.* primary shocks reflected off the clouds; as seen from Fig. 1 of NF , their contribution is less than 1% both for SNe and winds.

The distribution function $P_i^{(1)}(\mu)$ for primary shocks due to the i-th source, where $i = 1$ ($i = 2$) refers to SNe (winds), can be written as

$$P_i(\mathcal{M}) = \frac{4\pi}{3}\alpha_i\gamma_i\frac{R_{0i}^3}{V}\mathcal{M}^{-(\alpha+1)} = \frac{\alpha_i P_{0i}}{\mathcal{M}^{(\alpha+1)}}, \quad (6)$$

where $\mathcal{M}$ is the Mach number of the shock with respect to the intercloud gas supposed here to be at $T = 8000$ K and V is the volume affected by the energy input. The previous expression contains two parameters (R_{0i} and α_i) which completely define the self-similar stage of the shock radius evolution for the given source. Adopting the canonical values of NF, we take $R_{0i}/\mathrm{pc} = (70, 70)$ and $\alpha_i = (9/7, 9/2)$. The values for the radii of different turbulence sources (*i.e.* , isolated and clustered SNe, Winds, HII regions) are given in Table 1 of NF. In turn, the specific value of 70 pc is taken from Cioffi, McKee & Bertschinger (1988). The resultant primary shock distribution in the ISM is then

$$P(\mathcal{M}) = \sum_i \frac{P_{0i}}{\mu^{\alpha_i+1}} \quad (7)$$

From this distribution we randomly extract a value of the shock Mach number (or velocity, v_s); the velocity of the engulfed cloud before interaction with the shock, v_{c0}, is extracted from the actual PDF. The velocity acquired by the cloud in the direction of the shock propagation is (McKee & Cowie 1975, Miesch & Zweibel 1994)

$$v_{cs} = \left(\frac{\Delta}{\Delta+1}\right)\frac{v_{sh}}{\chi^{1/2}} , \quad (8)$$

where $\Delta = 4$ for an adiabatic shock and $\chi = 100$ is the canonical value for the density contrast between cloud and intercloud medium[†]. Thus the final velocity of the cloud after the interaction with the shock is

$$v_{ps}^2 = (v_{c0}^2 + v_{cs}^2 + 2v_{cs}v_{c0}\cos\zeta) , \quad (9)$$

where ζ is the angle between the directions of the shock propagation and the cloud motion before the interaction.

2.1.2 Kinetic energy dissipation in the collisions

Since the pioneering work of Spitzer, interstellar cloud collisions have always been considered as perfectly inelastic because, for typical Galactic clouds, the cooling time of the shocked gas is shorter than the characteristic time scale of the collision. Nevertheless, this assumption might be rather crude for small clouds and/or primordial galaxies where the gas metallicity is low and therefore the cooling time is longer. In a previous paper (RFM), we have investigated the dependence of the collision elasticity, ϵ_{cc}, defined as the ratio of the final to the initial kinetic energy of the clouds, on the velocity and mass ratio of the colliding clouds, metallicity and magnetic field strength. The problem has been studied via high-res numerical simulations. In the case of head-on collisions, RFM derived a handy analytical relationship that has been shown to correctly approximate the results of numerical simulations:

$$\eta_{cc} = 1 - \epsilon_{cc} = \frac{\Sigma_{cool}}{6n_cR_c} \propto \frac{v_r^3}{n_cR_c\Lambda(v_r, Z)} ; \quad (10)$$

Σ_{cool} is the column density of the post-shock radiative region, and Λ [erg cm^3 s^{-1}] is the gas cooling function. For

[†] $\chi = 100$ is an average value for the density contrast which is essentially derived by imposing pressure equilibrium between clouds and intercloud medium, as in the classical two-phase model scheme of the ISM. For small clouds this ratio can vary; however, the cloud velocity has only a mild, $\chi^{-1/2}$, dependence on its value.

clarity we summarize here the relevant results of RFM: (*i*) the kinetic energy dissipation in cloud collisions is minimum (i.e. the collision elasticity is maximum) for a cloud relative velocity $v_r \simeq 30$ km s^{-1}; (*ii*) the above minimum value is proportional ZR_c^2, where Z is the metallicity and R_c is the cloud size: the larger is ZR_c^2 the more dissipative (*i.e.* , inelastic) the collision will be; (*iii*) in general, we find that the energy dissipation decreases when the magnetic field strength and mass ratio of the clouds are increased and the metallicity is decreased, respectively.

In principle, molecular hydrogen cooling could be important, especially in a low metallicity gas. However, H_2 in diffuse gas is very easily photodissociated by stellar UV flux. Therefore we neglect to a first approximation the effects of such molecule on the elasticity.

In RFM we derived the elasticity for face-on collisions. We can estimate the mean elasticity of cloud collisions due to off-center encounters by assuming that the overlapping cloud area experiences a face-on collision whether in the rest of the cloud volume kinetic energy is conserved. With this simple hypothesis we obtain

$$\eta = 1 - \epsilon = \frac{\eta_{cc}}{2R_c} \int_0^{2R_c} \left(1 - \frac{b}{2R_c}\right)\, db = \frac{\eta_{cc}}{2}\ ; \qquad (11)$$

where η_{cc} is the energy dissipated for face-on collisions. With this definition, perfectly inelastic 3D collisions have a mean elasticity $\epsilon \simeq 0.5$. In Fig. 2 we show ϵ as a function of the cloud relative velocity, v_r, for clouds with metallicities $Z = 1, 0.1$ and 0.01 Z$_\odot$. We have assumed cloud temperature $T = 48K$, cloud radius $R_c = 0.5$ pc and cloud density given by eq. 19, derived form the assumption of pressure equilibrium of the multiphase ISM. The effect of magnetic field (neglected here) is both to increase the cross section of the collision and the elasticity of the face-on collision.

2.2 Selection of model parameters

As previously mentioned the parameters of our model can be fixed according to the derived observational constraints. For the Milky Way the values we adopt here are derived from data collected in Thronson & Shull (1990). The cloud gas number density is $n_c \approx 50$ cm^{-3} and the cloud radius is $R_c = 0.1 - 6$ pc; the cloud masses are therefore in the range $M_c \sim 0.0045 - 1000$ M$_\odot$. A typical atomic cloud has $R_c = 0.5$ pc and mass $M_c \sim 0.5$ M$_\odot$. Clouds with $M_c \gtrsim 1000$ M$_\odot$ are self-gravitating and we assume that they cannot remain in the atomic phase‡. The value of γ, expressing the number of cloud collisions between two subsequent SN explosions is in the range $1 - 1000$. The elasticity of the collision depends on the gas metallicity Z, the cloud radius R_c, and relative velocity v_r, according to eq. 11. Finally, we have adopted a SN rate of $\nu_{SN} = 0.04$ yr^{-1}. Note that once a value for γ is fixed, the SN rate determines the time step of the simulation but does not affect the properties of the PDF at equilibrium.

‡ Even clouds with $M_c \gtrsim 1000$ M$_\odot$ are fully molecular only in dense knots and should remain atomic in the outermost regions. But we neglect this complication.

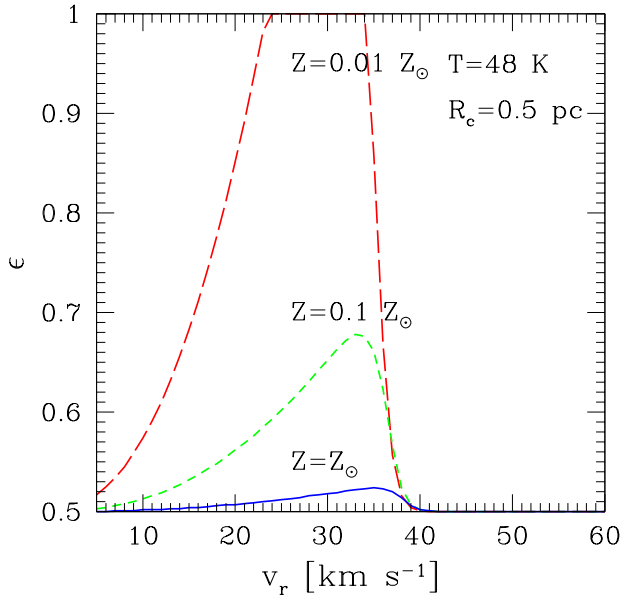

Figure 2. Elasticity of cloud collisions, ϵ, as a function of the cloud relative velocity, v_r, for clouds with metallicities $Z = 1, 0.1$ and 0.01 Z$_\odot$. By definition perfectly elastic collisions do not radiate away their initial kinetic energy because the shock propagating inside the clouds remains always adiabatic. The peak of the cloud collision elasticity at $v_r \sim 30$ km s^{-1} corresponds to maximum column density of the post-shock radiative region, $\Sigma_{cool} \propto v_r^3/\Lambda$. See text for more explanation.

3 RESULTS

3.1 A Test Case: Elastic Collisions

We have first tested our code on the perfectly elastic cloud collisions case. We have chosen several different initial conditions for the PDF, and in all cases, after a number of collisions comparable to the total number of clouds in the box, a stationary Maxwellian PDF is approached, as expected. The number of clouds and the total energy are conserved (in this case we set the energy input to zero) within less than 0.1%.

3.2 Constant Elasticity

We now assume that the initial PDF is Maxwellian with velocity dispersion $\sigma_M = 10$ km s^{-1} for all cases discussed below. We run several simulations exploring the effects of different values of γ, R_c, n_c and elasticity. The elasticity range is $0 \leqslant \epsilon \leqslant 1$ and in each simulation is set to a constant value unrelated to the physical properties of the clouds.

The typical number of collisions required to reach the stationary regime depends on the mean kinetic energy per cloud mass, $\langle E \rangle$, at the time when the stationary phase is reached: the lower is $\langle E \rangle$, the larger is the number of collisions required to reach the steady state. An example of a Monte Carlo simulation is shown Fig. 3.

The shape of the stationary PDF is well described by the parametric function

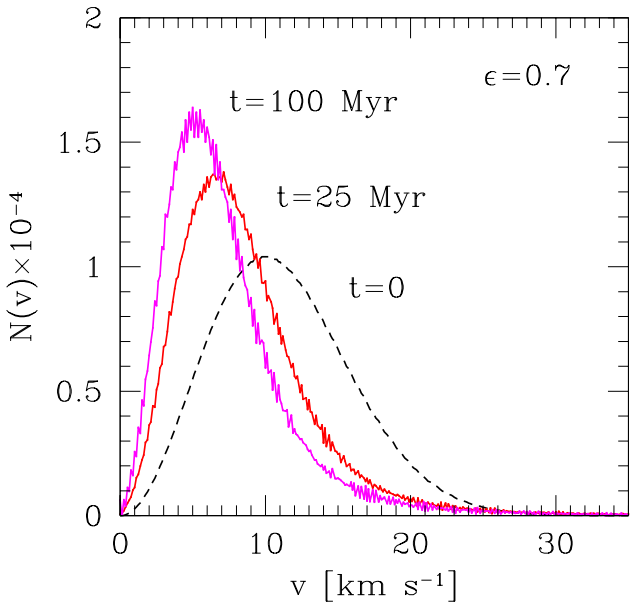

Figure 3. Evolution of the cloud velocity distribution, $N(v) = N_{tot}p(v)$, from a Monte Carlo simulation with $\epsilon = 0.7, \gamma = 110, R_c = 4.17$ pc, $M_c = 40$ M$_\odot$. The dashed line is the initial PDF, a Maxwellian distribution with $\sigma_M = 10$ km s^{-1}; the solid lines show the PDF at $t = 25$ and 100 Myr. For this run, a stationary PDF is reached after about 50 Myr.

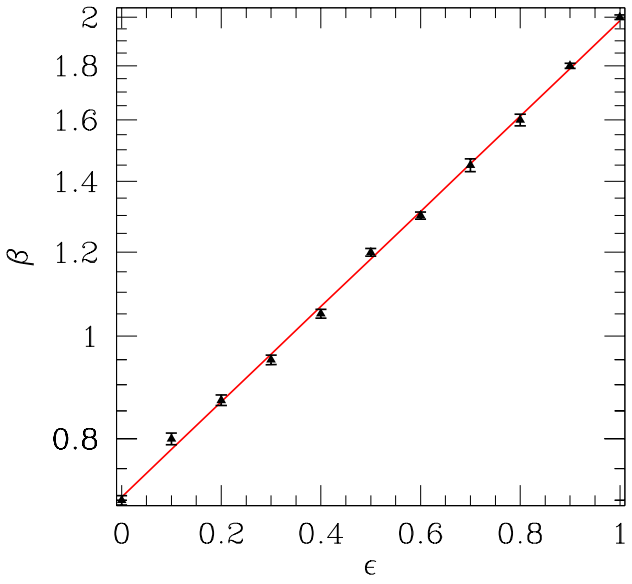

Figure 4. Shape of the PDF as a function of the elasticity. The parameter β in eq. (12) is a function of the elasticity ϵ only. The solid line shows the curve $\beta = 2\exp(\epsilon - 1)$: for elastic collisions ($\epsilon = 1$) the PDF is Gaussian, for inelastic collisions ($\epsilon = 0.5$) the PDF is close to exponential ($\beta = 1.2$).

$$p(v) = \frac{\beta}{\Gamma(3/\beta)\sigma}\left(\frac{v}{\sigma}\right)^2 \exp\left[-\left(\frac{v}{\sigma}\right)^\beta\right], \qquad (12)$$

whose maximum occurs at $v_{max} = (2/\beta)^\beta\,\sigma$. Here $\Gamma(x)$ is the gamma function. The distribution has total kinetic energy per unit mass

$$\langle E\rangle = \frac{\Gamma(5/\beta)}{\Gamma(3/\beta)}\sigma^2 \sim \frac{3}{2}\frac{1.05\sigma^2}{\beta - 0.947} \quad \text{if } 1 < \beta < 2\,. \qquad (13)$$

For the Maxwellian ($\beta = 2$), we have $\langle E\rangle = (3/2)\sigma_M^2$ and $\langle E\rangle = (3/40)\sigma^2$ if $\beta = 1$. In the range $1 < \beta < 2$ the function $\Gamma(5/\beta)/\Gamma(3/\beta) \approx 1.58/(\beta - 0.947)$.

We have performed several simulations to explore the effect of changes in the model parameters. If the mass of the clouds is not too large ($\gtrsim 1000$ M$_\odot$), the PDF is given by eq. (12), with the index β which is a function of the mean elasticity of the collisions only and independent on the details of the energy injection. However, in the case of massive clouds each collision dissipates an energy comparable to the energy injected by a typical SN explosion. Therefore, at the steady state, the number of cloud collisions per SN explosion is about one and the functional shape of the PDF depends on the SN energy input prescription. In Fig. 4 we show the tight correlation of β to the elasticity. The solid line, showing the best fit to the simulation points, has the simple expression

$$\beta = 2e^{(\epsilon-1)}\,, \qquad 0 \leqslant \epsilon \leqslant 1. \qquad (14)$$

For the perfectly inelastic case, according to eq. (11) $\epsilon = 0.5$, implying $\beta \simeq 1.2$.

A second conclusion can be drawn from our results. The mean kinetic energy per unit mass, $\langle E\rangle$, of the equilibrium distribution is simply related to the energy input per unit mass per cloud collision, $E_i = \kappa E_{SN}/\gamma M_c$, through the dissipation parameter $\eta = 1 - \epsilon$ by the following equation:

$$E_i = \eta\langle E\rangle = (1-\epsilon)\langle E\rangle = \frac{\Gamma(5/\beta)}{\Gamma(3/\beta)}\sigma^2 \ln\left(\frac{2}{\beta}\right) \qquad (15)$$

where we have used the two above relations. Eqs. (13)-(15) are useful to estimate ISM parameters, $\langle E\rangle, \epsilon$ and E_i from the observed shape of the PDF, characterized by β and σ. The typical value of M_c is a function of metallicity and will be derived in the next Section.

3.3 Physical Elasticity

We now use the more realistic prescription, eq. (11) for the elasticity of cloud-cloud collisions. The solid lines in Fig. 5 show the isocontours of constant β (left panel) and mean elasticity $\langle\epsilon\rangle$ (right panel) as a function of Z and R_c from the Monte Carlo simulations. The cloud gas density is $n_c = 50$ cm^{-3} and the temperature $T = 48$ K, the typical values for a two-phase ISM with $Z = Z_\odot$ (see RFM).

The value of β is found to be related to elasticity similarly to eq. 14, where now $\langle\epsilon\rangle$ is the mean elasticity. The latter is defined by

$$\begin{cases} \langle\epsilon\rangle = \int_0^\infty dv_r p(\sigma,\beta,v_r)\epsilon(v_r, Z, n_c, R_c) \\ \beta = 2e^{(\langle\epsilon\rangle-1)} \qquad 0.5 \leqslant \langle\epsilon\rangle \leqslant 1 \end{cases} \qquad (16)$$

where $p(\sigma,\beta,v_r)$ is the probability distribution function for the modulus of the relative velocity (rPDF). The values of β and $\langle\epsilon\rangle$, derived solving the system of eqs. (16), are shown in Fig. 5 (dashed lines).

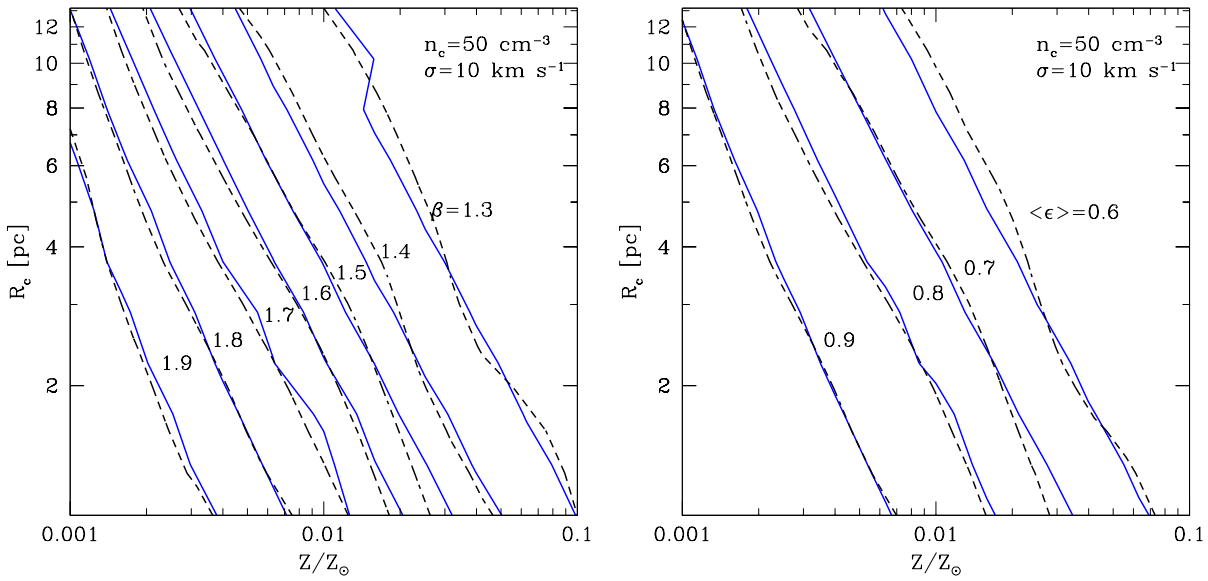

Figure 5. Isocontours of β (left) and mean elasticity $\langle\epsilon\rangle$ (right) as a function of gas metallicity Z and cloud size R_c. The solid lines refer to Monte Carlo simulation results; the dashed lines are the analytic solutions of eqs. 16. The cloud density is $n_c = 50$ cm^{-3}, the temperature $T = 48$ K and $\sigma = 10$ km s^{-1}.

The 1D rPDF is given by

$$p_{1D}(v_r) = \int dv_1 \int dv_2 p_{1D}(v_1) p_{1D}(v_2) \delta[v_r - (v_1 - v_2)] \quad (17)$$

Here, δ is the Dirac delta function and $p_{1D}(v) \propto \exp[-(v/\sigma_{1D})^\beta]$ is the normalized 1D PDF. It is easy to solve eq. (17) for the particular cases $\beta = 2$ and $\beta = 1$. For $\beta = 2$ the 1D rPDF is a Gaussian with $\sigma_r = \sqrt{2}\sigma$. In the $\beta = 1$ case, the rPDF is

$$p_{1D}(\sigma_{1D}, \beta = 1, v_r) = \frac{|v_r| + \sigma_{1D}}{4\sigma_{1D}^2} \exp\left(-\frac{|v_r|}{\sigma_{1D}}\right) \quad (18)$$

For arbitrary values of β eq. (17) has to be solved numerically. Eq. (18) shows that the functional form of the 1D rPDF and therefore the rPDF $p(\sigma, \beta, v_r)$ changes depending on β. Nevertheless, using Monte Carlo simulations we find that the parametric function $p(\sigma, \beta, v_r) \propto v_r^2 \exp[-(v_r/\sigma_r)^{\beta_r}]$ with $\sigma_r = \sigma(1 + \beta^{-3})2^{\frac{1}{\beta}}$ and $\beta_r = \beta(1 + 0.24\beta^{-3})$ is a good fit to rPDF. We have used this parameterization to solve the system of eqs. (16).

The mean elasticity, and therefore β, depend on σ. In Fig. 6 we show $\langle\epsilon\rangle$, calculated from eq. (16), as a function of σ for $Z = 5 \times 10^{-2} Z_\odot$ and $Z = 5 \times 10^{-3} Z_\odot$. The triangles show the analogous relation obtained from Monte Carlo simulations.

As discussed in § 2.1.2, cloud-cloud collisions are more elastic when their relative velocity is about 30 Km s^{-1}. This can be understood if we recall that the elasticity of the collision is proportional to the column density of the post-shock radiative region, $\Sigma_{cool} \propto v_s t_{cool} \propto v_s^3/\Lambda(T)$, where v_s is the shock velocity, t_{cool} the cooling time of the shocked gas and $\Lambda(T)$ is the gas cooling function. For small collision velocities the post-shock gas is cold ($T < 10^4$ K) therefore the cooling time is relatively long. In this regime the elasticity increases with the cloud relative velocity about as v_r^3. When the cloud relative velocity is high enough that the post-shock gas is heated above $T \sim 2 \times 10^4$ K, the cooling time becomes very short because of the Lyα cooling. Therefore the elasticity decreases steeply. The maximum of the mean elasticity $\langle\epsilon\rangle$ at $\sigma \approx 11$ Km s^{-1} is the consequence of the dependence of the cloud-cloud collision elasticity on the velocity of the clouds. In other words Σ_{cool} is maximum when $\sigma \approx 11$ Km s^{-1}.

The dependence of $\langle\epsilon\rangle$ on σ indicates that if $\sigma < \sigma_c \simeq 11$ km s^{-1} the PDF cannot reach a stationary state, *i.e.* an instability occurs. Physically, this is due to the fact that in this low-σ regime an increase (decrease) of σ produces an increase (decrease) of $\langle\epsilon\rangle$. As a result less (more) energy is dissipated and σ increases (decreases) further. The simulation results shown for this σ range do not reflect equilibrium values but are given at a time $t \sim 100$ Myr; eventually, depending on the parameters of the simulation the PDF relaxes either to the stable high-σ branch or to $\sigma \sim 0$. The time scale for this process is essentially given by the growth rate of the instability, which is particularly fast for a low metallicity gas and vanishes as Z is increased above $Z \approx 0.1 Z_\odot$. The growth rate of the instability is $\tau^{-1} \sim |E_i/\langle E\rangle - \langle\eta\rangle|\nu \propto (1 - \langle\epsilon\rangle)\nu$, where we remind that ν is the cloud collision rate. The triangles in the unstable region are evolved from the same Maxwellian PDF with $\sigma_M = 10$ km s^{-1} but with different values for E_i. The fact that the triangles in the unstable region lay very close to the solid line implies that eq. (15) is approximatively valid also when the system is not in a steady state. If $E_i < E_i^{crit} \sim 121[\Gamma(5/\beta^*)/\Gamma(3/\beta^*]\ln(2/\beta^*)$ km^2 s^{-2}, where $\beta^* = \beta(\sigma = 11)$ is a function of Z, M_c and n_c (see Fig. 7), the PDF will be unstable. Therefore, from Fig. 6 we conclude that in a multiphase, low metallicity ($Z \approx 5 \times 10^{-3} Z_\odot$) ISM the PDF should be close to a Maxwellian ($\beta = 2$) with velocity dispersion $\sigma \gtrsim 11$ km s^{-1}; in more metal rich systems ($Z \gtrsim 5 \times 10^{-2} Z_\odot$) instead we expect to observe an almost exponential tail of the PDF with $\beta \approx 1.2$. If $Z \gtrsim 0.1$, the instability of the PDF is not fast

enough to put strong constraints on the value of σ. We will discuss in § 4 the observational implications of these results.

Finally, we estimate the typical cloud mass as a function of the metallicity. As discussed in RFM, a multiphase ISM in thermal equilibrium can exist in a narrow range of thermal pressure. The pressure range depends on the gas metallicity but the temperature of the clouds (CNM) is $T \sim 48$ K, independent of the metallicity. This implies that exist a relationship between the cloud density n_c and Z. If we assume a cloud temperature $T = 48$ K and pressure equilibrium of the multiphase ISM we find

$$n_c(Z) \simeq n_c(Z=1)\exp[0.0834(Z^{-1/2}-1)]. \quad (19)$$

Adopting this relation we explore two different models:

Model A Since diffuse clouds are not self gravitating, we assume that their mass is a small (constant) fraction of the Jeans mass $M_J = (110 M_\odot) T^{3/2} n_c(Z)^{-1/2}$. The temperature of the cloud is approximately constant ($T = 48$ K), therefore the mass is $M_c \propto n_s(Z)^{-1/2}$ and the radius $R_c \propto n_c(Z)^{-1/2}$.

Model B Alternatively, we can derive the cloud size by imposing that the H_2 abundance in the cloud is negligible. If the cloud is optically thin to the H_2 photodissociating radiation in the Lyman-Werner bands (*i.e.* , has a column density $\Sigma_c = n(Z) R_c \lesssim (5\times10^{14}$ cm$^{-2})$), the H_2 abundance will be $x_{H_2} \lesssim 10^{-9}$ if the UV background in the galaxy has values comparable to the Milky-Way. We therefore assume that the column density of the clouds is a (constant) fraction of 5×10^{14} cm^{-2}. In this case we find the scaling laws: $R_c \propto n_c(Z)^{-1}$ and $M_c \propto n_c(Z)^{-2}$.

In Fig. 7 we show the maximum (at $\sigma = 11$ km s^{-1}) mean elasticity $\langle\epsilon\rangle$ as a function of the gas metallicity, Z. The three solid lines show the mean elasticity assuming that cloud masses scale with metallicity as $M_c(Z) = M_c(Z=1)[n_c(Z)/n_c(Z=1)]^{-1/2}$ for $M_c(Z=1) = 0.1, 1, 10$ M$_\odot$ (*i.e.* , Model A). The dashed lines show the analogous relation assuming $M_c(Z) = M_c(Z=1)[n_c(Z)/n_c(Z=1)]^{-2}$ for $M_c(Z=1) = 0.1, 1, 10$ M$_\odot$ (*i.e.* , Model B). The mean elasticity increases when the gas metallicity decreases as a consequence of the lower cooling rate of metal-deficient gas. When the mass of the clouds is small the mean elasticity is larger because of the smaller cloud column density, Σ_c (we have seen in § 2.1.2 that the cloud-cloud collision elasticity is inversely proportional to Σ_c). The difference between models A and B is also caused by the dependence of the cloud column density on the gas metallicity. In Model A $\Sigma_c(Z) \propto n_c(Z)^{1/2}$ and in Model B $\Sigma_c(Z)$ is constant.

4 OBSERVATIONAL LINKS

The results presented above allow to make a number of predictions concerning the ISM velocity PDF which can be tested against observations. The first attempts to determine the PDF of the ISM date back to the early 50s. These studies used optical absorption lines toward OB stars or HI 21 cm emission or absorption line to measure the velocity PDF of local gas at distances $d \lesssim 1$ kpc. More recently the question of the velocity PDF has received much less attention. In the following, we will briefly summarize the available observational results; we particularly emphasize the point that the large majority of them indicate that a exponential PDF

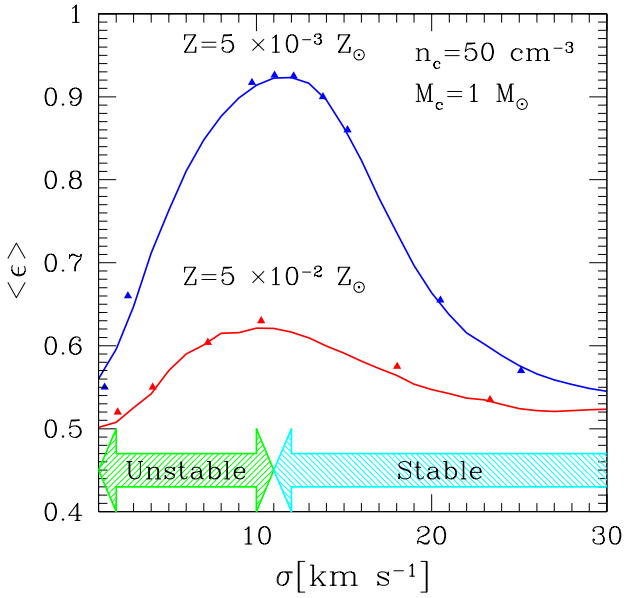

Figure 6. Mean elasticity $\langle\epsilon\rangle$, as a function of cloud velocity dispersion σ. The solid lines show the analytical result obtained by solving eq. (16) for $Z = 5\times10^{-2} Z_\odot$ and $Z = 5\times10^{-3} Z_\odot$ (small integration errors are responsible for the wavy appearance of the lower line). The triangles show the analogous relation as obtained from Monte Carlo simulations. It can be shown that if $\sigma < \sigma_c \simeq 11$ km s^{-1}, the PDF is unstable.

at large σ is a much better fit than a Gaussian one to the velocity data.

Adams (1949) compiled a catalog including 230 Ca K absorption line velocities produced by "clouds" along the line of sight to nearby OB stars. He found 150 components towards 120 stars with $d < 500$ pc and 80 components towards 43 stars with $d > 500$ pc. Using such catalog, Blaauw (1952) and Takakubo (1967), showed that a single exponential could fit the velocity PDF of local interstellar clouds better than a single Gaussian. Analyzing the same data, Huang (1950) and Kaplan (1954) preferred a fit with a v^{-1} function; Siluk & Silk (1974) fitted the high-velocity tail of the PDF with a v^{-3} function. Another set of optical interstellar lines, toward 132 stars was observed by Munch (1957). He used a different method, the "doublet ratio method" (Ca H and K or NaD2/D1). His conclusions confirm Blaauw's results.

Mast & Goldstein(1970) observed the radial velocities of a sample of 268 HI 21 cm emission clouds. In order to clearly resolve the clouds in velocity, they chose a sample of high latitude line of sights and estimate the peculiar velocity distribution after correction for solar motion and differential galactic rotation. It is evident from their Fig. 4 that an exponential fits better the data than a Gaussian. Falgarone and Lequeux (1973), using data from Radhakrishnan *et al.* (1972 a,b,c,d), Goss & Radhakrishnan (1972) and Hughes, Thompson & Colvin (1971) analyzed the PDF of the ISM in the solar neighborhood. Their results are in agreement with those of Mast & Goldstein(1970) but their sample is too limited to discriminate the detailed shape of

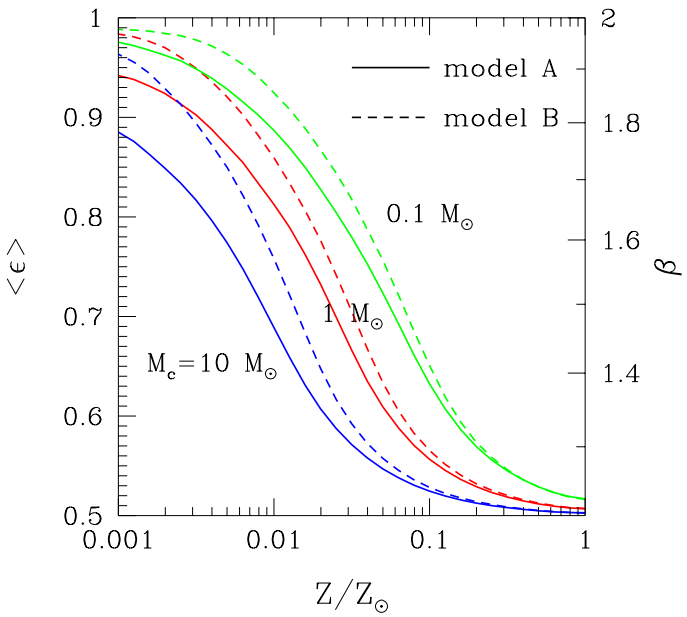

Figure 7. Mean elasticity $\langle\epsilon\rangle$, as a function of the metallicity Z (normalized to the solar metallicity), for $\sigma = 11$ km s^{-1}. We assume that the clouds are in pressure equilibrium in a multiphase medium. This assumption imply that the clouds have temperature $T = 48$ K and density $n_c(Z) \simeq n_c(Z=1)\exp[0.0834(Z^{-1/2}-1)]$ (*i.e.* , $P(Z) = n_c T \simeq P(Z=1)\exp[0.0834(Z^{-1/2}-1)]$, where $P(Z=1) = 2400$ cm^{-3} K). Here we assume $n_c(Z=1) = 50$ cm^{-3}. The solid lines show the mean elasticity assuming that cloud masses scale with metallicity as $M_c(Z) = M_c(Z=1)[n_c(Z)/n_c(Z=1)]^{-1/2}$ for $M_c(Z=1) = 0.1, 1, 10$ M$_\odot$ (Model A). The dashed lines show the analogous relation assuming $M_c(Z) = M_c(Z=1)[n_c(Z)/n_c(Z=1)]^{-2}$ for $M_c(Z=1) = 0.1, 1, 10$ M$_\odot$ (Model B). The rationale for models A and B is explained in the text.

the distribution. Crovisier (1978) studied the kinematics of nearby HI clouds using the Nancay 21-cm absorption survey (Crovisier *et al.* 1978). The sample consisted of about 300 cloud radial velocities. They also confirmed that the 1D PDF is close to exponential, although their conclusion suffers of possible contamination from a population of intermediate-velocity clouds. Dickey, Terzian, & Salpeter (1978) obtained the radial velocity distribution of clouds from the Arecibo 21-cm emission/absorption survey. Unfortunately, the statistics is too small to clearly discriminate the functional form of the PDF. Kim *et al.* (1998) measured the PDF for motions out of the plane of the Large Magellanic Cloud. The peculiar velocity PDF, on scales larger than 15 pc, is well fitted by an exponential.

In a slightly different context, Miesch, Scalo & Bally (1999) estimated the PDF of molecular line centroid velocity fluctuations for several nearby molecular clouds with active internal star formation. The data consist of over 75,000 ^{13}CO line profiles divided among 12 spatially and/or kinematically distinct regions. These regions range in size from less than 1 to more than 40 pc and show substantially supersonic motions. They find that 3 regions (all in Mon R2) exhibit nearly Gaussian centroid PDFs, but the other 9 show nearly exponential PDFs.

In spite of this impressive amount of evidences, many authors have continued to make the assumption when modeling or interpreting ISM data that the velocity PDF for the diffuse and molecular clouds is Gaussian. This bias is probably due to the expectations from incompressible turbulence models of the ISM, which predict that the PDF is nearly Gaussian. For systems whose metallicity is larger than about 1/20 of solar, our model predicts instead that the velocity PDF should approximate an exponential distribution. The physical reason for this discrepancy resides in the dissipative nature of cloud collisions. From our results, an exponential PDF can only be obtained if the ensemble averaged elasticity is 0.5, indicating perfectly inelastic collisions. Hence, kinetic energy stored in turbulent motions is efficiently converted in thermal energy and radiated away in shocks arising in colliding flows. The (supersonic) turbulence decays very rapidly and a corresponding high rate of energy deposition is required to stir the gas. This is in agreement with the findings of up-to-date numerical simulations in the context of star formation (e.g. Smith, MacLow & Heitsch 2000; Padoan & Nordlund 1999).

Finally, we would like to comment on the dynamical instability discussed above (see Fig. 6). If values of σ corresponding to the unstable $\sigma < 11$ km s^{-1} region are deduced from observations of a low metallicity system, because of the runaway character of the instability, σ should rapidly decrease or increase assuming a constant SN energy injection rate. If σ decreases, leading to a loss of pressure support and hence to overall contraction, is likely to drive a similarly rapid increase of the star formation rate and energy injection from SN explosions. This will cause σ to start increasing. An increasing σ will lead to overall expansion of the ISM and the star formation rate and the SN energy injection will decrease back to the the starting value. Therefore σ starts decreasing again unless the energy injection rate is sufficient to maintain $\sigma > 11$ km s^{-1}. As a result a "bursty" star formation mode will occur, unless σ is increased up to the stable region, thus stabilizing the star formation rate on a higher level. The period of the burst cycle should increase with the gas metallicity because the timescale of the instability does. A "bursty" mode of star formation has indeed been observed in some low surface brightness (LSB) dwarf galaxies (Schombert, McGaugh & Eder 2001). Thus, the dynamical instability occurring together with the dissipation of kinetic energy investigated here might provide an interesting self-regulation of the star formation activity in low-metallicity and low surface brightness galaxies. The suggested self-regulation mechanism is rather speculative given the simplicity of our model and should be tested using more realistic numerical simulations.

5 DISCUSSION

Turbulent supersonic flows and gas self-gravitation create structures in the ISM that are very complex and hierarchically structured. It is still under debate whether interstellar clouds are only transient phenomena produced by dynamical fluctuations or can be represented as long-living clouds. Numerical simulations (Wada, 2001) and observa-

tions (Schwarz & van Woerden, 1974) show that the morphology of the atomic component of the ISM is a complex network of filamentary structures. The filaments are probably produced by oblique shock collisions and shear from differential galactic rotation. The typical size of the filaments in the simulations is about 1 pc, consistent with the observed typical size of atomic interstellar clouds. Contrary to self-gravitating molecular clouds, the atomic clouds do not show evident substructures.

In our simple toy model clouds do not coalesce or are destroyed, and their mass, size and number density remain constant. Our assumptions are not physically justified but are the correct choice for a statistical description of the ISM.

The outcome of slow inelastic collisions could produce cloud coalescence. If this process is important, eventually the cloud mass reaches the Jeans mass and the atomic cloud becomes a self-gravitating molecular cloud. Perhaps this process, in conjunction with fragmentation of dense gas shells produces by SN explosions, is responsible for the regulation of the gas ratio between the atomic and molecular phases of the ISM. Simulations show that small clouds are probably destroyed if they are passed by supersonic shocks. In this process mass is exchanged between atomic clouds and the intercloud diffuse gas. Indeed from numerical simulations it is evident that clouds are not long lived entities but instead they are continuously formed and destroyed. But despite the complex and time dependent morphology of the ISM, statistical analysis of the cloud properties in numerical simulations shows that the typical cloud size, cloud mass, and cloud number density have constant equilibrium values (Wada & Norman, 2001). Therefore our model is not physically realistic but our simple assumptions are justified in a statistical sense. For this reason we cannot study the ISM morphology or the physics that regulates mass exchange between different phases of the ISM. But we believe that our model is reliable for a statistical study of kinetic energy dissipation in "cloud" collisions. At least on scales where the isotropy assumption in the ISM holds.

Because of the aforementioned arguments, we suspect that adding complexity to the model (for instance assuming non homogeneous density clouds or a cloud mass spectrum) would not help substantially in making the results more realistic and reliable. Nevertheless, in a work currently in preparation, we are using 2D high-resolution hydrodynamic simulations to model the ISM in galaxies with primordial (metal-poor) composition. These simulations should be able to test the quality of the results presented in this paper.

Finally we discuss to which extent the results of this work can be extended to different systems, namely subclumps in molecular clouds and when the main turbulent energy source is different from SN explosions.

Observations of the velocity PDF in molecular cloud cores (Miesch, Scalo & Bally, 1999) have shown that the 1D PDF is better represented by an exponential rather than Gaussian distribution. Based on the results of our model, that applies to atomic clouds, we have suggested that kinetic energy dissipation in collision of sub-clumps is at the origin of the exponential velocity distribution. Even if we believe that an analogy between atomic clouds in the ISM and sub clumps in molecular clouds is possible, we have to keep in mind important differences. Molecular clouds, are self gravitating and harbor smaller clumps for which size-mass-velocity relations have been derived from observations (*e.g.*, Larson, 1981). The inter-clump gas can be atomic especially in the outermost regions. Our assumption of homogeneity and isothermality for clouds of same sizes and the derived scalings can serve as a first-order approach to the real hierarchically structured molecular cloud. More important, in our model we do not include molecular chemistry and cooling. Note that, if molecular hydrogen is not dissociated, clump collisions are inelastic (because of radiative cooling from collisionally excited H_2 rotational and vibrational levels) even if the gas has primordial composition (metal-free).

One of the results discussed in § 3 is that the shape of the PDF does not depend on the kinetic energy input prescription if the energy input event (SN explosion in our case) is much larger than the energy dissipated by a typical collision event. This means that our results should remain valid even if the main kinetic energy source that fuels the ISM turbulence is not SN explosions. Stellar winds are are important energy sources. Chimney and superbubbles created by multiple SN explosions in a stellar cluster can reduce the amount of energy input in the ISM and produce, instead, gas outflows from the ISM to the intergalactic medium. Finally Wada & Norman (1999) have shown that the rotational energy of the disk is converted into turbulent energy of the ISM because of the combined effects of gas self-gravity and disk differential rotation.

6 SUMMARY

We have investigated the kinetic energy of the ISM in galaxies as a function of their gas metallicity. We use a simple closed model where the energy injection from SN explosions balance the energy dissipated in cloud collision. Using Monte Carlo simulations, coupled with a simple (but statistically motivated) model for the clouds and previous numerical results on the elasticity of collisions derived by RFM, we have been able to link the properties of the velocity PDF with the ISM kinetic energy dissipation. In particular, we find that:

• The slope, β, of the velocity PDF only depends on the value of the ensemble averaged elasticity $\langle\epsilon\rangle$ as $\beta = 2\exp(\langle\epsilon\rangle - 1)$.

• The knowledge of β and of the velocity dispersion σ of the gas allows to determine the specific kinetic energy input from SNe, E_i through the simple relation $E_i \approx 1.58\sigma^2 \ln(2/\beta)/(\beta - 0.947)$; in steady state, this input is equal to the energy dissipated by collisions.

• We predict that (see Fig. 6) in a multiphase, low metallicity ($Z \approx 5 \times 10^{-3} Z_\odot$) ISM the PDF should be close to a Maxwellian ($\beta = 2$) with velocity dispersion $\sigma \gtrsim 11$ km s^{-1}; in more metal rich systems ($Z \gtrsim 5 \times 10^{-2} Z_\odot$), instead we expect to observe exponential PDFs with $\beta \approx 1.2$.

• We have pointed out that, contrary to what is usually assumed, the available data firmly allow to conclude that the Galactic ISM velocity PDF is not Gaussian but has rather an exponential shape. This is in perfect agreement with our predictions.

• Low metallicity systems with $\sigma < 11$ km s^{-1} are dynamically unstable on time scales $\tau \propto [(1-\langle\epsilon\rangle)\nu]^{-1}$ where ν is the cloud collision rate. This systems are probably undergoing a "bursty" mode of star formation. Indeed, some observations suggest that LSB dwarf galaxies show signs of re-

peated and weak bursts of star formation which shape their irregular morphology appearance (Schombert, McGaugh & Eder 2001). On the contrary, a quiescent star formation mode as inferred for the Milky Way, should be associated with an ISM velocity dispersion $\sigma \approx 11$ km s^{-1} and a relatively high star formation rate.

REFERENCES

Adams, W. S. 1949, ApJ, 109, 354
Ballesteros-Paredes, J., Vázquez-Semadeni, E. & Scalo, J. 1999, ApJ, 515, 286
Blaauw, A. 1952, Bull. Astron. Inst. Netherlands, 11, 459 (B52)
Cioffi, D. F., McKee, C. F., & Bertschinger, E. 1988, ApJ, 334, 252
Crovisier, J. 1978, A&A, 70, 43
Crovisier, J., Kazes, I. & Aubry, D. 1978, A&AS, 32, 205
Dickey, J. M., Terzian, Y. & Salpeter, E. E. 1978, ApJS, 36, 77
Falgarone, E. & Lequeux, J. 1973, A&A, 25, 253
Ferrara, A. 1993, ApJ, 407, 157
Ferrara, A. & Tolstoy, E. 2000, MNRAS, 313, 291
Goss, W. M., Radhakrishnan, V., Brooks, J. W. & Murray, J. D. 1972, ApJS, 24, 123
Hennebelle, P. & Pérault, M. 1999, A&A, 351, 309
Huang, S. S. 1950, ApJ, 112, 399
Hughes, M. P., Thompson, A. R. & Colvin, R. S. 1971, ApJS, 23, 323
Kaplan, S. A. 1954, Soviet Astron., 31, 137
Katz, N. 1992, ApJ, 391, 502
Kim, S., Staveley-Smith, L., Dopita, M. A., Freeman, K. C., Sault, R. J., Kesteven, M. J., & McConnell, D. 1998, ApJ, 503, 674
Korpi, M. J. *et al.* 1999, ApJL, 514, 99
Larson, R. B. 1981, MNRAS, 194, 809
Lockman, F. J. & Gehman, C. S. 1991, ApJ, 382, 182
Mast, J. W. & Goldstein, S. J. 1970, ApJ, 159, 319
McKee, C.F. & Cowie, L. L. 1975, ApJ, 195, 715
McKee, C.F. 1990, in The Evolution of the Interstellar Medium, ed. L. Blitz, (San Francisco:PASP), 3
Miesch, M. S., Scalo, J. & Bally, J. 1999, ApJ, 524, 895
Miesch, M. S. & Zweibel, E. 1994, ApJ, 432, 622
Mihos, J. C. & Hernquist, L. 1994, ApJ, 437, 611
Miniati, F., Jones, T. W., Ferrara, A. & Ryu, D. 1997, ApJ, 491, 216
Miniati, F. Ryu, D., Ferrara, A. & Jones, T. W. 1999, ApJ, 510, 726
Munch, G. 1957, ApJ, 132, 319
Navarro, J. F. & Steinmetz, M. 2000, ApJ, 538, 477
Norman, C. A. & Ferrara, A. 1996, ApJ, 467, 280 (NF)
Padoan, P. & Nordlund, A. 1999, ApJ, 526, 279
Radhakrishnan, V., Brooks, J. W., Goss, W. M., Murray, J. D. & Schwarz, U. J. 1972a, ApJS, 24, 1
Radhakrishnan, V., Murray, J. D., Lockhart, P. & Whittle, R. P. J. 1972b, ApJS, 24, 15
Radhakrishnan, V., Goss, W. M., Murray, J. D. & Brooks, J. W. 1972c, ApJS, 24, 49
Radhakrishnan, V. & Goss, W. M. 1972d, ApJS, 24, 161
Ricotti, M., Ferrara, A. & Miniati, F. 1997, ApJ, 485, 254 (RFM)
Rosen, A. & Bregman, J. M. 1995, ApJ, 440, 634
Rosen, A. , Bregman, J. M., & Norman, M. L. 1993, ApJ, 413, 137
Rosen, A., Bregman, J. M. & Kelson, D. D. 1996, ApJ, 470, 839
Schombert, J. M., McGaugh, S. S. & Eder, J. A. 2001, AJ, in press (astro-ph/0101458)
Siluk, R. S., & Silk, J. 1974, ApJ, 192, 51
Smith, M. D., Mac Low, M.-M. & Heitsch, F. 2000, A&A, 362, 333
Springel, V. 2000, MNRAS, 312, 859
Schwarz, U. J. & van Woerden, H. 1974, IAU Symp. 60: Galactic Radio Astronomy, 60, 45
Takakubo, K. 1967, Bull. Astron. Inst. Netherlands, 19, 125
Thronson, H. A. & Shull, J. M. 1990, ASSL Vol. 161: The Interstellar Medium in Galaxies,
Thornton, K., Gaudlitz, M., Janka, H.-Th. & Steinmetz, M. 1998, ApJ, 500, 95
Vazquez-Semadeni, E., Passot, T. & Pouquet, A. 1995, ApJ, 441, 702
Vazquez-Semadeni, E., Cantó, J. & Lizano, S. 1998, A&A, 492, 596 702
Wada, K. 2001, ApJL, 559, L41
Wada, K. & Norman, C. A. 2001, ApJ, 547, 172
Wada, K. & Norman, C. A. 1999, ApJL, 516, L13